Optimisation of distributed feedback laser biosensors

J. Coote, S. Reddy and S.J. Sweeney

Abstract: A new integrated optical sensor chip is proposed, based on a modified distributed-feedback (DFB) semiconductor laser. The semiconductor layers of different refractive indices that comprise a laser form the basis of a waveguide sensor, where changes in the refractive index of material at the surface are sensed via changes in the evanescent field of the lasing mode. In DFB lasers, laser oscillation occurs at the Bragg wavelength. Since this is sensitive to the effective refractive index of the optical mode, the emission wavelength is sensitive to the index of a sample on the waveguide surface. Hence, lasers are modelled as planar waveguides and the effective index of the fundamental transverse electric mode is calculated as a function of index and thickness of a thin surface layer using the beam propagation method. We find that an optimised structure has a thin upper cladding layer of $\sim 0.15\ \mu$m, which according to this model gives detection limits on test layer index and thickness resolution of 0.1 and 1.57 nm, respectively, a figure which may be further improved using two lasers in an interferometer-type configuration.

1 Introduction

A biosensor is a sensing device that employs a biological agent such as a protein, DNA strand or cell as a selective detector. Since biochemical interactions are often highly specific, it is possible to create a sensing surface coated with a particular 'sensing' molecule, where a reaction will only take place in the presence of the molecule's target reactant. A good example of this is the enzyme electrode [1], one of the first biosensors, where the enzyme glucose-oxidase is the sensing element for glucose molecules. Optical biosensors are those that measure the response of the biological sensing element using light. One approach is to use the spectrum of laser light resonating in a cavity to examine the biomolecular composition of fluids and cells within the cavity, as described by Gourley [2]. Another approach of particular interest is 'evanescent field' sensing. The evanescent field of a guided wave is highly sensitive to refractive index changes at the surface of a waveguide, so can be used to detect very small changes in the refractive index and thickness of a surface layer. Techniques often used in biochemical research include fibre-optic chemical sensing [3], surface plasmon resonance [4] and dual-polarisation interferometry [5]. The latter two may be implemented as a label-free system, that is, not requiring the use of fluorescent dyes, as is the case with many optical biosensing systems. However, the resolution of such systems is determined by the physical size of the instruments: hence, they tend to be large and costly, as well as being laboratory based only. There is a widespread demand for biochemical sensors that are compact and cost-effective, in addition to

being highly sensitive, for 'in the field' applications such as medical diagnostics and security detection. Optical sensors based on dielectric waveguides and grating couplers have been investigated by Lukosz [6], and more recently work has been published on biophotonic devices based on semiconductor lasers such as that by Cohen *et al.* [7, 8]. This approach is attractive, since semiconductor lasers provide us with a ready-made integrated optical chip containing a light source and waveguide. In this paper, we present an approach whereby 1.55 μm InGaAsP/InP distributed-feedback (DFB) lasers can be adapted to use as integrated biosensor chips. Waveguide simulations are carried out using the beam propagation method (BPM) [9] with a view to finding an optimum structure both for sensing and laser performance.

2 Sensing using DFB lasers

An evanescent field sensor exploits the fact that changes in the refractive index of the material within the mode volume of a guided wave will alter the propagation of the wave, and hence the modal effective index. Therefore a change in the index of material at the interface between a waveguide and the surrounding medium may be sensed because of the presence of the evanescent field that extends into the cladding medium. Such a sensor can then be used as a refractometer to detect changes in the index of a bulk medium (e.g. a chemical solution) flowed over the sensing surface, or for monitoring the formation of a thin film on the sensing surface, for example, the binding of an analyte to immobilised antibodies [6]. The resulting changes in effective index can be observed as a change in phase, amplitude, in- or out-coupling angle or wavelength depending on the type of sensor [3–8].

In a DFB laser, optical feedback is provided by a Bragg reflection grating, allowing amplification only at the Bragg wavelength. It can be shown that the Bragg wavelength, λ, is proportional to the modal effective index, μ_{eff} [10]

$$\frac{\Delta\mu_{\text{eff}}}{\mu_{\text{eff}}} = \frac{\Delta\lambda}{\lambda} \tag{1}$$

J. Coote and S.J. Sweeney are with the Advanced Technology Institute, University of Surrey, Guildford GU2 7XH, UK

S. Reddy is with the School of Biomedical and Molecular Science, University of Surrey, Guildford GU2 7XH, UK

E-mail: j.coote@surrey.ac.uk

where $\Delta\mu_{\text{eff}}$ is the change in effective index and $\Delta\lambda$ the change in the Bragg wavelength.

By modification of the laser structure to allow the optical mode to interact with material at the surface of the laser chip, we should be able to observe a change in lasing wavelength in response to changes in the refractive index of this surface material, and hence create an integrated optical sensor chip.

3 Waveguide simulations

The critical factor in determining the sensitivity of an evanescent field sensor is the optical power contained in the sensing region [11]. To optimise this, we investigated the ways in which laser structures could be modified to increase sensitivity. Separate confinement heterostructures (SCH) were modelled as planar waveguides consisting of a thick InP substrate layer, a thin InGaAsP layer forming the SCH, which contains the active region and is referred to here as the 'waveguide layer', and a cladding layer of InP. A thin 'test layer' was added to the surface to represent a layer of adsorbed biomolecules.

Waveguide structures were designed using RSoft Photonics CAD Suite [12], and the mode-solving program BeamPROP was used to calculate the effective index of the fundamental transverse electric mode as a function of the refractive index and thickness of the test layer. Sensitivity was then defined as $d\mu_{\text{eff}}/d\mu_t = S_\mu$ or $d\mu_{\text{eff}}/dt = S_t$, where μ_t and t are the refractive index and the thickness of the test layer, respectively.

Three ways of modifying the laser structure were considered: (1) changing the refractive index of the waveguide layer, thereby altering the index step $\Delta\mu$ between the waveguide core and the cladding layers; (2) changing the thickness l of the upper cladding layer and (3) adding an extra 'mode stretching' high-index layer to the structure, located between the waveguide core and the test layer at a distance l_1 from the upper edge of the waveguide core. Cross sections and transverse refractive index profiles for the various structures investigated are shown in Fig. 1. Refractive index values for InP and InGaAsP are taken from [13].

4 Results from mode solving

Plots of the calculated effective index against test layer index and thickness are shown in Fig. 2, for a three layer waveguide with $\Delta\mu = 0.23$. In the range applicable to protein monolayers, that is, $0 < t \leq 5$ nm and $1 \leq \mu_t \leq 2$ (where $t = 0$ nm and $\mu_t = 1$ relate to an absence of
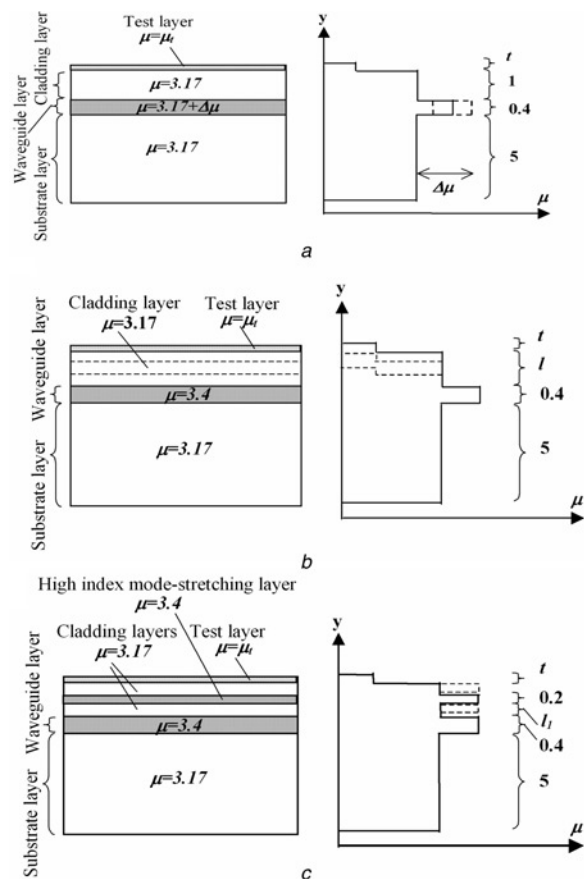

Fig. 1 *Cross sections and refractive index profiles of waveguides investigated (all lengths in µm)*

Variable quantities are:
a $\Delta\mu$ = refractive index step
b l = cladding layer thickness
c l_1 = separation of waveguide and mode-stretching layers

adsorbed molecules, and a background index of 1 is assumed), these curves are approximately linear, so we estimate the sensitivity of the effective index to the test layer index and the thickness by fitting a straight line to the curve in this range and taking the gradient. These gradient values are plotted as functions of the parameters being varied in Figs. 3–5. An increase in sensitivity is brought about both by reducing the index step $\Delta\mu$ between the waveguide core and the cladding layers and by thinning the upper cladding layer (reducing l). In case of the structure with the mode-stretching layer, maximum sensitivity is obtained when the high-index layer is positioned midway between the waveguide core and the test layer.
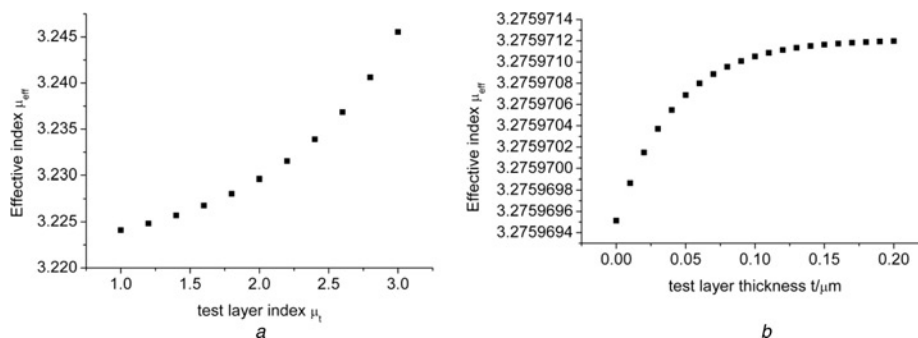

Fig. 2 *Effective index for a three layer waveguide with $l = 1$ µm and $\Delta\mu = 0.23$*
Versus
a Test layer index
b Test layer thickness

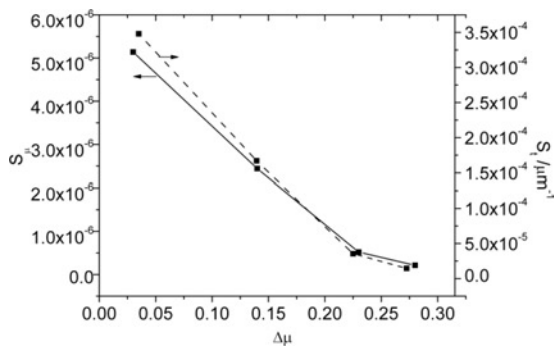**Fig. 3** *Sensitivity of a three-layer waveguide sensor with $l = 1$ μm against refractive index step $\Delta\mu$*

Reducing the index step between the core and the cladding layers from 0.28 to 0.03 results in a 24-fold increase in sensitivity, from 1.46×10^{-5} to 3.48×10^{-4} μm^{-1} for S_t, and from 2.14×10^{-7} to 5.14×10^{-6} for S_μ.

Thinning the upper cladding layer from $l = 1$ to 0 μm increases the sensitivity by three orders of magnitude: from 3.55×10^{-5} to 3.73×10^{-2} μm^{-1} for S_t, and from 5.20×10^{-7} to 5.48×10^{-4} for S_μ it should however be noted that the complete removal of the p-cladding layer is not practicable in a real laser – Section 5). Addition of the high-index layer at a distance of 0.4 μm from the waveguide core yields values of $S_\mu = 3.04 \times 10^{-6}$ and $S_t = 2.07 \times 10^{-4}$ μm^{-1}. These values are summarised in Table 1, which also shows the improvements in sensitivity relative to a standard laser structure. The standard structure in question is taken to be a three-layer waveguide with a difference in refractive indices between the waveguide core and the cladding layers $\Delta\mu = 0.23$, an upper cladding layer thickness $l = 1$ μm and with calculated sensitivity of $S_t\{\text{standard}\} = 3.55 \times 10^{-5}$ μm^{-1}, $S_\mu\{\text{standard}\} = 5.2 \times 10^{-7}$. From Table 1, we can see that of the approaches considered here the most effective way to improve sensing performance is to thin the upper cladding layer.

In order to explain these results, we refer to the plots shown in Fig. 6. The result of lowering the index step in a waveguide is to reduce the optical confinement, so that more power resides in the evanescent field (Fig. 6a and b). Thinning the upper cladding layer brings the test layer into closer proximity with the waveguide layer. Since the evanescent field in the cladding layer decays exponentially with distance, this clearly increases the power in the test layer (Fig. 6c and d). Finally, placing a thin high-index layer within the upper cladding layer has the expected
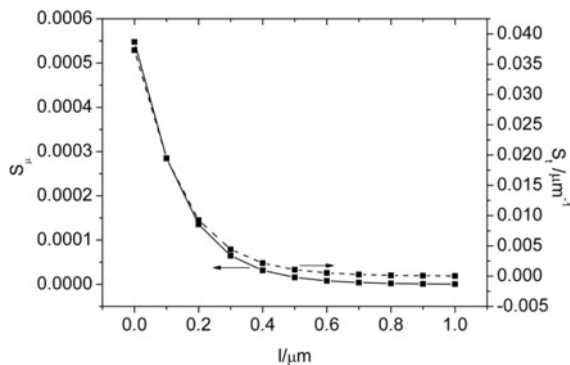

Fig. 4 *Sensitivity of a three-layer waveguide sensor with $\Delta\mu = 0.23$ against cladding layer thickness l*
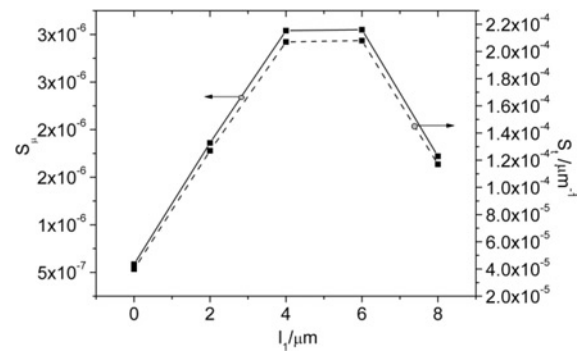

Fig. 5 *Sensitivity of a five-layer waveguide sensor with $\Delta\mu = 0.23$ against separation distance of waveguide and mode-stretching layer (l_1)*
Total thickness of the cladding and mode-spacing layers is fixed at 1 μm

result of stretching the optical mode, resulting in a stronger evanescent field in the test layer (Fig. 6e and f).

The mode profiles also suggest that the first approach (reducing the index step) would be unsuitable for modification of semiconductor lasers, since the lower refractive index step leads to a reduced confinement of the optical field and injected carriers, and would significantly increase the laser threshold (although this is not the primary concern for this application). Optical confinement will also be an important factor to determine the optimum thickness of the cladding layer if the second approach (thinning the cladding layer) is to be employed (see Section 5).

5 Confinement factor

Clearly, it would be impracticable to thin the cladding layer indefinitely, because the upper p-doped layer of a laser is required both for carrier injection and for wave guiding. The effect on laser performance was evaluated by calculating the confinement factor as a function of cladding layer thickness, where confinement factor is defined as the fraction of the total integrated power contained within the laser active region. In these simulations, only the transverse confinement factor is considered, since the slab is assumed to be infinite in the horizontal (x) direction and the propagating field can be approximated to a plane wave. The laser threshold gain α_{th} is given by [14]

$$\alpha_{\text{th}} = \frac{1}{\Gamma}\left(\Gamma_{\text{ac}} + (1 - \Gamma)\alpha_{\text{ex}} + \frac{1}{L}\ln\left(\frac{1}{R}\right)\right) \qquad (2)$$

where Γ is the confinement factor, α_{ac} and α_{ex} the optical losses in the active and external regions, respectively, L the length of the cavity and R the reflectivity of the laser facets. From (2), we can see that reducing the confinement factor will lead to an increase in lasing threshold. Fig. 7 shows a plot of the confinement factor against cladding layer thickness for a three-layer waveguide with index step $\Delta\mu = 0.23$, assuming the active region to be a 20 nm thick layer located in the centre of the waveguide layer, and assuming a constant n-cladding layer thickness of 5 μm. For the purposes of modelling the confinement factor, a passive waveguide was assumed, with no absorption or gain. The curve has a maximum at $l = 0.15$ μm, indicating an optimum p-cladding layer thickness of this value. Further calculations showed that the refractive index and thickness of the test layer had a negligible effect on Γ. Also with an absorption term included in

Table 1: Maximum sensitivities obtained through different structural modifications

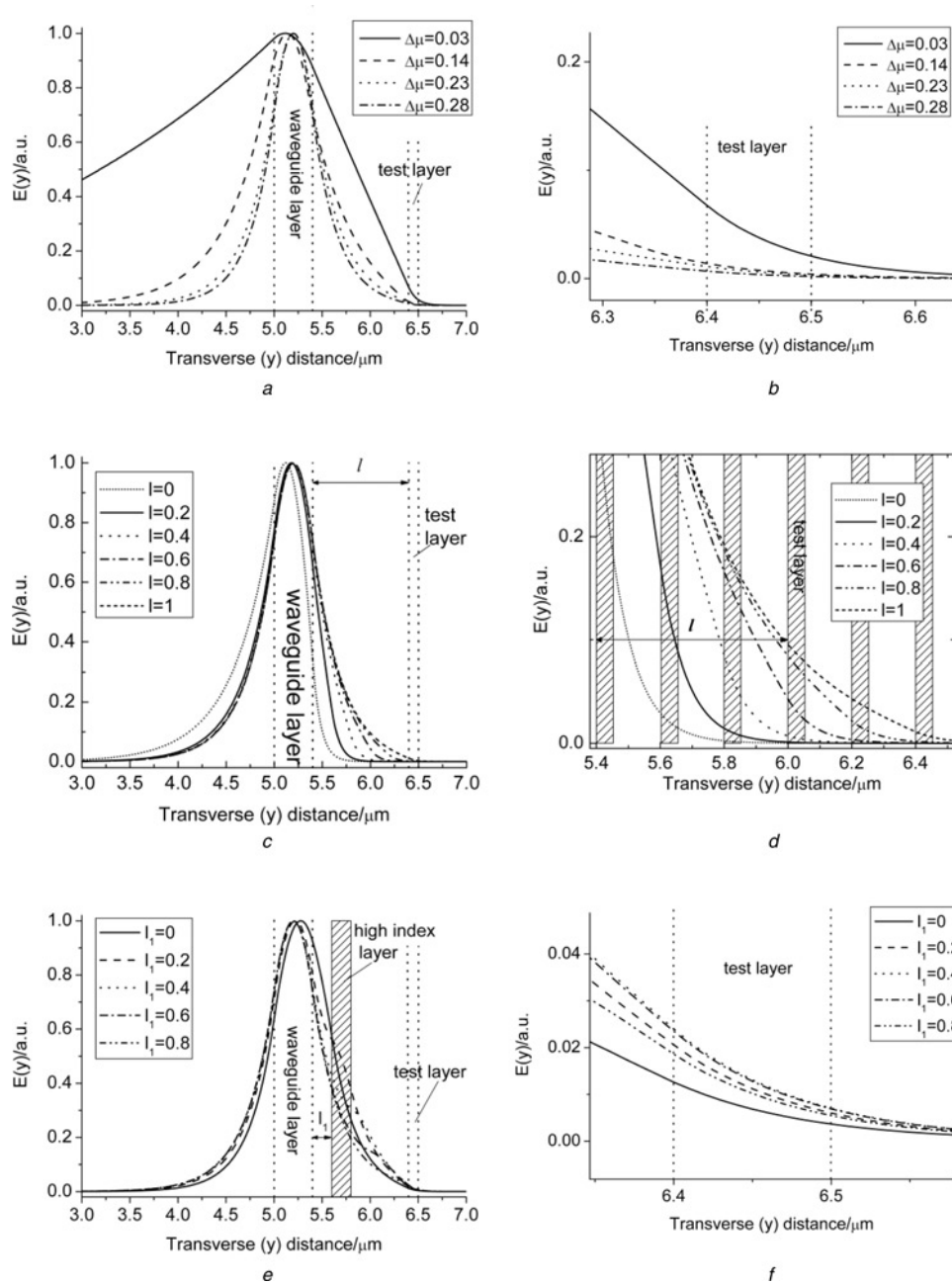| Structure	S_μ	$S_t/\mu m$	S_μ/S_μ {standard)} and $(S_t/S_t$ {standard})
three-layer waveguide, $\Delta\mu = 0.23$, $l = 1\ \mu m$ (standard)	5.20×10^{-7}	3.55×10^{-5}	1 (1)
three-layer waveguide, $\Delta\mu = 0.03$, $l = 1\ \mu m$	5.14×10^{-6}	3.48×10^{-4}	9.88 (9.80)
three-layer waveguide, $\Delta\mu = 0.23$, $l = 0\ \mu m$	5.48×10^{-4}	3.73×10^{-2}	1050 (1050)
five-layer waveguide, $\Delta\mu = 0.23$, $l = 1\ \mu m$, $l_1 = 0.4\ \mu m$	3.04×10^{-6}	2.07×10^{-4}	5.84 (5.84)

Fig. 6 *Mode profiles for the fundamental TE mode in the waveguide structures investigated*

Left panel shows the transverse mode profile $E_x(y)$ in the waveguide and cladding layers and right panel shows an enlarged view of the same plots in the test layer region
a and *b* Index step is the parameter
c and *d* Upper cladding layer thickness is the parameter
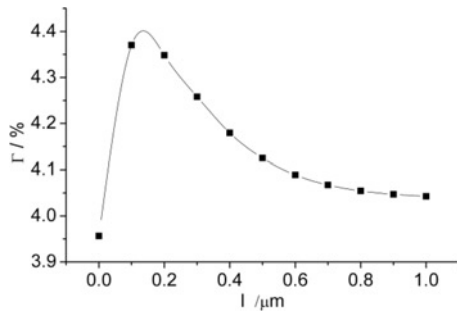*e* and *f* Distance between waveguide and mode-stretching layers is the parameter

Fig. 7 *Confinement factor as a function of cladding layer thickness for three-layer waveguide with $\Delta\mu = 0.23$*

the refractive index of the test layer, the calculated effective index values were shifted by a maximum difference of the order 10^{-5}, but there was no significant change in the sensitivities or confinement factor. In this model, we assume a slab waveguide, but the working sensor will be based on a DFB grating, and so the effects of the test layer on the coupling coefficient κ will need to be taken into account in future models. We would expect κ and hence the threshold gain to increase as a function of effective index, but a detailed calculation is beyond the scope of the present work.

6 Sensor performance

The results presented here suggest that a laser device optimised for both sensing performance and optical confinement could be achieved by reducing the upper cladding layer thickness to $\sim 0.15\ \mu m$. Effective index is plotted for this structure against test layer index and thickness in Fig. 8, giving an estimated sensitivity of $S_\mu = 1.97 \times 10^{-4}$ and $S_t = 1.34 \times 10^{-2}\ \mu m^{-1}$. The calculated effective index when $t = 0.005\ \mu m$ and $\mu_t = 1.45$ is 3.25913. Assuming a minimum detection limit on wavelength shifts of $\Delta\lambda = 0.01$ nm with a standard laboratory wave meter; from (1) we obtain a minimum detectable effective index change

$$\Delta\mu_{\text{eff}} = \mu_{\text{eff}} \times \frac{\Delta\lambda}{\lambda} = 3.25913 \times \frac{1 \times 10^{-11}}{1.55 \times 10^{-6}}$$
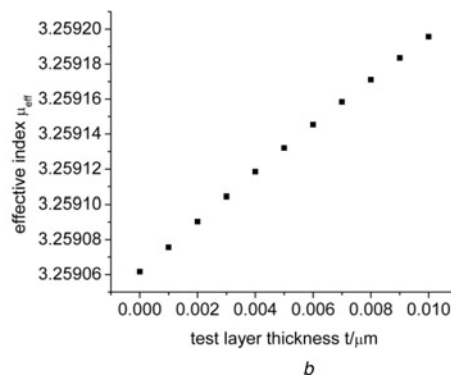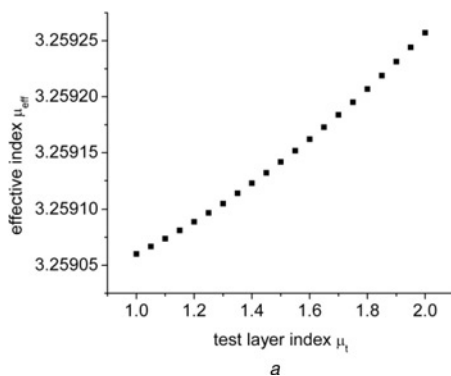$$= 2.1 \times 10^{-5}$$

Taking the sensitivity values quoted above, we can estimate the detection limits on test layer index and thickness:

$$\Delta(\mu_t, t)_{\min} = \left(\frac{d\mu_{\text{eff}}}{d(\mu_t, t)}\right)^{-1} \Delta\mu_{\text{eff}_{\min}},$$

$$\Delta t_{\min} = \frac{2.1 \times 10^{-5}}{1.34 \times 10^{-2}} = 1.57\ \text{nm},$$ (3)

$$\Delta\mu_{t_{\min}} = \frac{2.1 \times 10^{-5}}{1.97 \times 10^{-4}} = 0.1$$

For the purposes of monitoring an adsorbing protein monolayer, we assume that the layer thickness remains constant while the density increases. We can then translate the detection limit calculated above into surface mass density using (4), which is derived from a formula used in [15]

$$\Delta M_{\min} = \frac{t}{d\mu_t/d\rho} \Delta\mu_{t_{\min}}$$ (4)

where ΔM is the change in surface mass density in g/cm^2 and $d\mu_t/d\rho$ is the differential change in refractive index of the adsorbed layer with density. Taking $d\mu_t/d\rho$ to be a constant 0.182 g/cm^2 [15] and $t = 0.005\ \mu m = 5 \times 10^{-7}$ cm, we obtain

$$\Delta M_{\min} = \frac{5 \times 10^{-7}}{0.182} \times 0.1 = 0.27\ \mu g/cm^2$$

To improve upon this sensitivity, it should be possible to use a pair of identical lasers, acting as the sensing and reference arms in an optical interferometer-type configuration. The signal is then the difference between the two wavelengths, which can be measured as the beat frequency between the two laser beams using an electrical spectrum analyser. This interference frequency is given by the frequency difference between the two signals

$$\Delta f = c\left(\frac{1}{(\lambda + \Delta\lambda)} - \frac{1}{\lambda}\right)$$ (5)

where c is the speed of light in a vacuum. An easily measurable frequency difference of $\Delta f = 100$ MHz corresponds to a wavelength shift of 0.8 pm with $\lambda = 1550$ nm, according to (5). Inserting this value into (1), we obtain $\Delta\mu_{\text{eff min}} = 1.7 \times 10^{-6}$, and from (3), we then obtain $\Delta\mu_{t\ \min} = 8.6 \times 10^{-3}$ and $\Delta t_{\min} = 0.13$ nm, an improvement of one order of magnitude on the previously calculated value. Equation (4) then gives $\Delta M_{\min} = 24$ ng/cm^2. This can be converted into a molar concentration by dividing

Fig. 8 *Effective index against test layer index*

a Thickness
b Optimised waveguide structure

by the adsorbed layer thickness (here assumed to be 5 nm) and the molar mass of the target molecule. Bovine serum albumin (BSA), a protein molecule commonly used in biosensor studies has a relative molecular mass of 67 kD; we therefore obtain a molar concentration of 7.1×10^{-4} M as the detection limit for BSA. Using twinned lasers has also been shown to dramatically reduce the noise caused by temperature-induced wavelength drift in the DBR-based sensor chips demonstrated by Cohen *et al.* [8]. In an interferometer-type configuration, we predict that the detection limits may be improved by at least one order of magnitude, enabling detection of adsorbed layers of the order 100 pm thick and surface mass densities of 24 ng/cm^2. The two lasers, operating simultaneously, should be subject to the same environmental fluctuations, resulting in only the wavelength shifts because of refractive index changes being detected. In a working sensor, we envisage the sample being delivered by a microfluidic system, or alternatively the sensor could be used in a non-liquid environment, for example, in gas sensing, where a polymer coating is used to selectively absorb gas molecules.

7 Conclusion

We have investigated a new type of integrated optical sensor based on an InP/InGaAsP DFB laser chip, which uses the evanescent field in the upper layers of the laser waveguide to sense changes in refractive index at the surface of the chip. The advantages of such a sensor would be sensitivity, compactness and the relative simplicity of adapting readily available commercial laser devices for this purpose. The sensors were modelled as planar waveguides with a thin layer of biological material on the surface. To evaluate sensitivity, the effective refractive index of the waveguide was calculated using the BPM, as a function of the refractive index and thickness of the thin biological layer. The most sensitive waveguide was found to be that with the thinnest possible upper cladding layer, and an optimum design was proposed, based on this fact and calculations of the optical confinement factor, which is relevant to laser performance. The proposed structure has an upper cladding layer thickness of 0.15 μm, and the detection limits on test layer index and thickness are found to be 0.1 and 1.57 nm, respectively. Finally, we predict that if two lasers are used in an interferometer-type configuration, these detection limits may be improved by at least one order of magnitude offering great potential for highly sensitive and specific miniature photonic biosensors.

9 References

1 Updike, S.J., and Hicks, G.P.: 'The enzyme electrode', *Nature*, 1967, **214**, pp. 986–988
2 Gourley, P.L.: 'Biocavity laser for high-speed cell and tumour biology', *J. Phys. D: Appl. Phys.*, 2003, **36**, pp. 228–239
3 Andrade, J.D., Vanwagenen, R.A., Gregonis, D.E., Newby, K., and Lin, J.N.: 'Remote fibre-optic biosensors based on evanescent-excited fluoro-immunoassay: concept and progress', *IEEE Trans. Electron. Dev*, 1985, **32**, (7), pp. 1175–1179
4 Jönsson, U., Fägerstam, L., Ivarsson, B., *et al.*: 'Real-time biospecific interaction analysis using surface plasmon resonance and a sensor chip technology', *Biotechniques*, 1991, **11**, (5), pp. 620–627
5 Cross, G.H., *et al.*: 'The metrics of surface adsorbed small molecules on the Young's fringe dual-slab waveguide interferometer', *J. Phys. D: Appl. Phys.*, 2004, **37**, pp. 74–80
6 Lukosz, W.: 'Integrated optical chemical and direct biochemical sensors', *Sensor. Actuat. B-Chem.*, 1995, **29**, pp. 37–50
7 Cohen, D.A., Skogen, E.J., Marchand, H., and Coldren, L.A.: 'Monolithic chemical sensor using heterodyned sampled grating DBR lasers', *Electron. Lett.*, 2001, **37**, (22), pp. 1358–1360
8 Cohen, D.A., Nolde, J.A., Pedretti, A.T., Wang, C.S., Skogen, E.K., and Coldren, L.A.: 'Sensitivity and scattering in a monolithic heterodyned laser biochemical sensor', *IEEE J. Sel. Top. Quant.*, 2003, **9**, (5), pp. 1124–1131
9 Scarmozzino, R., Gopinath, A., Pregla, R., and Helfert, S.: 'Numerical techniques for modelling guided-wave photonic devices', *IEEE J. Sel. Top. Quant.*, 2000, **6**, (1), pp. 150–162
10 Carroll, J., Whiteaway, J., and Plumb, D.: 'Distributed feedback semiconductor lasers' (The Institution of Electrical Engineers, London, 1998)
11 Tiefenthaler, K., and Lukosz, W.: 'Sensitivity of grating couplers as integrated-optical chemical sensors', *J. Opt. Soc. Am. B*, 1989, **6**, (2), pp. 209–220
12 RSoft Photonics CAD Suite Version 5.1.0.2 and BeamPROP Copyright© 1993–2003 (RSoft Design Group)
13 Adachi, S.: 'Refractive indices of III-V compounds: key properties of InGaAsP relevant to device design', *J. Appl. Phys.*, 1982, **53**, (8), pp. 5863–5869
14 Asada, M., Adams, A.R., Stubkjaer, K.E., Suematsu, Y., Itaya, Y., and Arai, S.: 'The temperature dependence of the threshold current of GaInAsP/InP DH lasers', *IEEE J. Quant. Electron.*, 1981, **17**, (5), pp. 611–619
15 Vörös, J.: 'The density and refractive index of adsorbing protein layers', *Biophys. J.*, 2004, **87**, pp. 553–561